JAMES | Journal of Advances in Modeling Earth Systems

RESEARCH ARTICLE
10.1029/2021MS002470

A Model of C_4 Photosynthetic Acclimation Based on Least-Cost Optimality Theory Suitable for Earth System Model Incorporation

Helen G. Scott[1] **and Nicholas G. Smith**[1]

[1]Texas Tech University, Lubbock, TX, USA

Key Points:

- A parameter-sparse model of C_4 photosynthetic acclimation to changes in environmental conditions based on photosynthetic least cost theory
- Including acclimation will improve simulations of C_4 carbon assimilation and water/nutrient-use efficiencies under present/future conditions
- In simulated competition experiments with a similar C_3 model, C_4 photosynthesis becomes less advantageous under increased carbon dioxide

Supporting Information:

Supporting Information may be found in the online version of this article.

Correspondence to:

H. G. Scott,
helengracescott@gmail.com

Citation:

Scott, H. G., & Smith, N. G. (2022). A model of C_4 photosynthetic acclimation based on least-cost optimality theory suitable for Earth System Model incorporation. *Journal of Advances in Modeling Earth Systems*, *14*, e2021MS002470. https://doi.org/10.1029/2021MS002470

Received 13 JAN 2021
Accepted 2 FEB 2022

Abstract Empirical studies have shown that plant photosynthetic responses to environmental change can vary over time due to acclimation, but acclimation responses are often not included in Earth System Models. Photosynthetic least cost theory can be used to develop models of photosynthetic acclimation that are simple and testable. The theory is based on the idea that plants will acclimate to minimize the ratio of carbon costs to photosynthetic assimilation rate (Prentice et al., 2014, https://doi.org/10.1111/ele.12211). Formulations of this theory have been developed for C_3 plants, but not C_4 plants, which account for over 20% of global photosynthesis and are over-represented among widely grown crops. Here, we use photosynthetic least cost theory to derive a model for C_4 photosynthetic acclimation to above-ground abiotic conditions. We then compare our model's responses to a similar model of C_3 photosynthetic acclimation and find that C_4 photosynthesis has the highest simulated advantage over C_3 photosynthesis in hot, dry, and low CO_2 environments. We find that this advantage predicts C_4 abundance globally, but that the shallower CO_2 response of C_4 as compared to C_3 photosynthesis will reduce C_4 plant competitiveness under future conditions, despite higher temperatures. We also show that an acclimated model predicts similar or faster rates of C_4 under all conditions than a model that does not consider acclimation, suggesting that Earth System Models (ESMs) are underestimating future C_4 carbon uptake by not including acclimation. Our model is designed for easy incorporation into such ESMs.

Plain Language Summary Plants change their rate of photosynthesis in response to their environment. Their photosynthetic rates can change minute to minute based on the quick changes in their environment, but they can also change over much longer timescales as the plants become accustomed to a new environmental condition. Long-term (days to weeks) regulation of photosynthesis is termed acclimation. When we predict how plants will behave in the future, we must take acclimation into account so that we can more accurately predict the future carbon, water, and nutrient cycles. Previous studies have developed mathematical models of photosynthetic acclimation for some, but not all, plants. One understudied group of plants that lacked an acclimation model were the C_4 species, a subtype of plants often found in deserts and other arid environments, but one that also includes important agricultural crops such as maize. In this study, we develop a theoretical model of photosynthetic acclimation for C_4 species and show that the model yields expected results based on where C_4 plants currently grow. Our model can improve the predictions of carbon, water, and nutrient cycling in larger Earth System Models.

1. Introduction

Current Earth System Models (ESMs) are highly sensitive to the representation of photosynthetic processes and their response to environmental conditions (Booth et al., 2012). These models commonly predict photosynthetic process rates based on instantaneous responses (i.e., seconds to minutes; Smith & Dukes, 2013). However, decades of empirical studies have shown that plants adjust their responses when subjected to longer-term (days to weeks) changes in environmental conditions, due to acclimation (Bazzaz, 1990; Berry & Bjorkman, 1980; Boardman, 1977; Dusenge et al., 2019; Smith & Dukes, 2013; Way & Yamori, 2014; Yamori et al., 2014). Previous studies have shown that including C_3 photosynthetic acclimation alters biophysical and biogeochemical feedback in ESMs (Friend, 2010; Kattge & Knorr, 2007; King et al., 2006; Lombardozzi et al., 2015; Mercado et al., 2018; Smith et al., 2016, 2017; Thornton et al., 2007a; Zaehle & Friend, 2010). However, there is no acclimation model for plants that use the C_4 photosynthetic pathway.

Photosynthetic acclimation has been observed for C_4 species (Bellasio & Griffiths, 2014; Dwyer et al., 2007; Sage, 1999; Smith & Dukes, 2017; Yamori et al., 2014) and may occur through changes in both stomatal (Bellasio & Griffiths, 2014; Maherali et al., 2002) and biochemical (Sage & Kubien, 2007; Smith & Dukes, 2017) processes. However, it is essential to note that these acclimation responses may differ from those observed in C_3 species (Maherali et al., 2002; Yamori et al., 2014). For instance, the mesophyll cells of C_4 leaves contain phosphoenolpyruvate carboxylase (PEPc), which captures incoming CO_2 and shuttles carbon to ribulose-1,5-bisphosphate carboxylase/oxygenase (RuBisCO) in specialized bundle sheath cells (Kanai & Edwards, 1999). The high concentration of carbon shuttled to the bundle sheath cells increases the relative amount of carboxylation versus oxygenation that RuBisCO performs (Kanai & Edwards, 1999). Because of this specialized anatomy, C_4 species operate at lower stomatal conductance rates than C_3 species and show a reduced sensitivity of photosynthetic processes to CO_2, temperature, and vapor pressure deficit (Sage, 1999). High CO_2 concentrations in the bundle sheath and the Kranz anatomy may partially explain C_4 species difficulty to fully acclimate to changing conditions as quickly as C_3 species (Maherali et al., 2002; Sage & McKown, 2006; Yamori et al., 2014). However, there are not many experimental comparisons available in the literature.

In complement to empirical studies, theoretical models of photosynthetic functioning can help elucidate the mechanisms underlying environmental responses (Collatz et al., 1991, 1992; Ehleringer et al., 1997; Farquhar et al., 1980; Wang et al., 2017; Zhou et al., 2018). Classic work has used these models to compare simulated photosynthetic rates of C_3 and C_4 species under varying environmental conditions as a way of explaining geographic patterns in the abundance of species utilizing different photosynthetic pathways (Ehleringer et al., 1997). Other studies have used theoretical models to predict historical ranges of C_4 plants at geologic timescales (Zhou et al., 2018). These studies have confirmed C_4 advantages in warm, arid, high light, and low CO_2 environments. However, these studies have either omitted acclimation (Ehleringer et al., 1997) or only included simplified empirical representations of acclimation processes (Zhou et al., 2018). The recent development of theoretical models for C_3 photosynthetic acclimation (Wang et al., 2017) presents the opportunity to perform similar theoretical comparisons between C_3 and C_4 species while accounting for acclimation with the complimentary development of a theoretical model for C_4 photosynthesis.

Here, we develop a novel theoretical model of C_4 photosynthetic acclimation to above-ground environmental conditions. The model is based on the least-cost theory of photosynthesis (Wright et al., 2003), extending the original theory based on C_3 species to C_4 species. The least-cost hypothesis states that plants will acclimate to minimize the carbon costs to assimilate carbon through photosynthesis on a per-leaf-area basis (Prentice et al., 2014). The combined carbon costs include the costs of carboxylation and transpiration (Prentice et al., 2014; Wang et al., 2017). Carboxylation incurs a carbon cost due to the creation and maintenance of proteins, including RuBisCO (Wang et al., 2017). Here, C_4 plants may incur a greater carbon cost, due to the need to maintain additional enzymes, including PEPc. Transpiration incurs a carbon cost because of the need to maintain living tissues to support water transport (Wang et al., 2017). By minimizing costs, the photosynthetic assimilation rate is maximized per carbon cost so the least cost hypothesis could also be called a maximum photosynthetic efficiency hypothesis. We develop the model using a similar approach to Wang et al. (2017) and use it to predict acclimated values for intracellular CO_2, photosynthetic biochemistry, and photosynthesis of C_4 leaves under varying environmental conditions.

We use the theoretical model to compare responses to environmental conditions in leaves under acclimated and non-acclimated conditions to explore potential impacts the model might have on carbon uptake if included in an ESM. We also replicate classical theoretical competition experiments (Ehleringer et al., 1997) to explore the conditions under which C_4 species have greater carbon assimilation rates than C_3 species.

2. Methods

We developed this theoretical model of C_4 photosynthetic acclimation by combining the coordination theory of photosynthetic biochemistry (Maire et al., 2012; J.-L. Chen et al., 1993) and the least-cost hypothesis of stomatal conductance (Prentice et al., 2014; Wright et al., 2003). The primary assumption is that optimally acclimated plants will minimize the ratio of carbon costs to photosynthetic assimilation rate (Prentice et al., 2014). Figure 1 shows a schematic representation of the model.

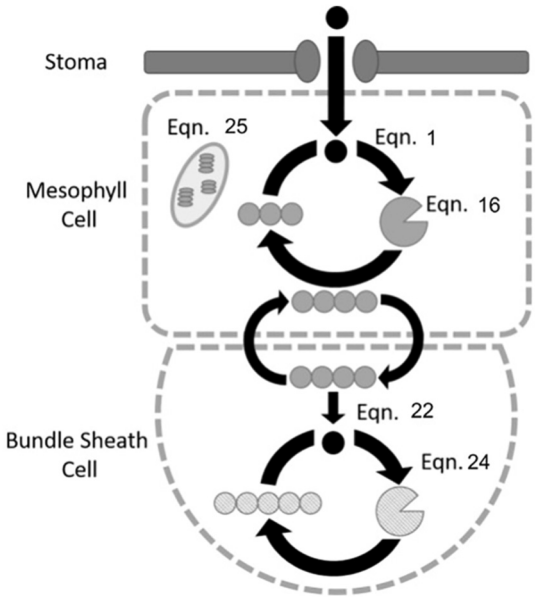

Figure 1. Schematic representation of the main features of the acclimated C_4 model. CO_2 diffuses into the mesophyll cell, where it is fixed into a C_4 acid by PEPc at the rate of V_{pmax}. The C_4 is concentrated in the bundle sheath at the rate of g_{bs}, where it is unpackaged, and fixed by RuBisCO at the rate of V_{cmax}. The rate of the electron transport chain (J_{max}) limits PEP and RuBP regeneration. Arrows indicate the path of molecule diffusion.

The least-cost hypothesis predicts the optimal ratio of intercellular CO_2 (C_i) to atmospheric CO_2 (C_a), referred to here as χ_m. We then use χ_m to estimate the concentration of CO_2 in the mesophyll cell (C_m) and the bundle sheath cell (C_{bs}). These CO_2 concentrations, along with the growing season conditions of light available for photosynthesis (photosynthetically active radiation, or PAR) and temperature, serve as inputs to calculate the maximum rates of carboxylation by PEPc (V_{pmax}) and RuBisCO (V_{cmax}) as well as electron transport (J_{max}). First, we present a theoretical model to estimate χ_m, parameterized with a worldwide data set of isotope discrimination in C_4 plants. We then describe how we use the coordination theory to predict optimal J_{max}, V_{pmax}, and V_{cmax}.

2.1. Optimal C_m Calculation

We developed a modified version of the C_3 least-cost model from Prentice et al. (2014) for C_4 plants to calculate the partial pressure of CO_2 present in the mesophyll cells (C_m (Pa)). We calculate C_m as a fraction of atmospheric CO_2 (c_a (Pa)).

$$C_m = \chi_m c_a \tag{1}$$

χ_m is the ratio of atmospheric to mesophyll CO_2, we define it as:

$$\chi_m = \frac{\xi}{\xi + \sqrt{D}}, \text{where } \xi = \sqrt{\frac{\beta K_p}{1.6\eta^*}} \tag{2}$$

where D is the vapor pressure deficit (Pa), K_p is the Michaelis-Menten constant for for PEPc (Pa), and η^* is the viscosity of water relative to its value at 25°C ($\eta^* = \eta/\eta_{ref}$; unitless).

The value β (unitless) in Equation (2) is the ratio (b/a) of dimensionless cost factors for maintaining carboxylation (b) to maintaining transpiration (a). We use a value of 166 for β, which was fit to a world-wide data set of carbon isotope discrimination values for C_4 species (Cornwell et al., 2018). This β value is in contrast to the β value for C_3 plants, 240 (Wang et al., 2017).

Here, we assumed that the C_m was equal to the intercellular CO_2 (C_i). This will correspond to infinite mesophyll conductance, where there is no resistance to the movement of CO_2 from the intercellular space into mesophyll cells.

One key difference between Equation (2) and the original C_3 version is the assumption that no mesophyll photorespiration is occurring in C_4 plants. Because of this simplification, there are no terms in this equation dependent on atmospheric CO_2 levels. The effects of this assumption are shown and discussed later with Figure 2. For the full derivation of Equation (2), see the Supporting Information S1.

2.2. Coordination Hypothesis

The rate of C_4 photosynthetic assimilation (A) is the minimum value of possible photosynthetic rates limited by different factors (Collatz et al., 1992; Von Caemmerer, 2000; Von Caemmerer & Furbank, 1999). The three primary limiting rates for C_4 photosynthesis are: (1) electron transport rate-limited photosynthesis (A_L), limited by enzymes that use PAR to drive the electron transport chain that regenerates PEP and RuBP, (2) PEPc limited photosynthesis (A_P), limited by the rate of carboxylation by PEPc, and (3) RuBisCO limited photosynthesis (A_C), limited by the rate of RuBisCO carboxylation. The rate of photosynthesis (A) in C_4 plants can be represented as:

$$A = \min\{A_L, A_P, A_C\} \tag{3}$$

The coordination hypothesis states that under acclimated conditions, optimal leaf biochemistry will lead to equal rates of (A_L), (A_P), and (A_C) or

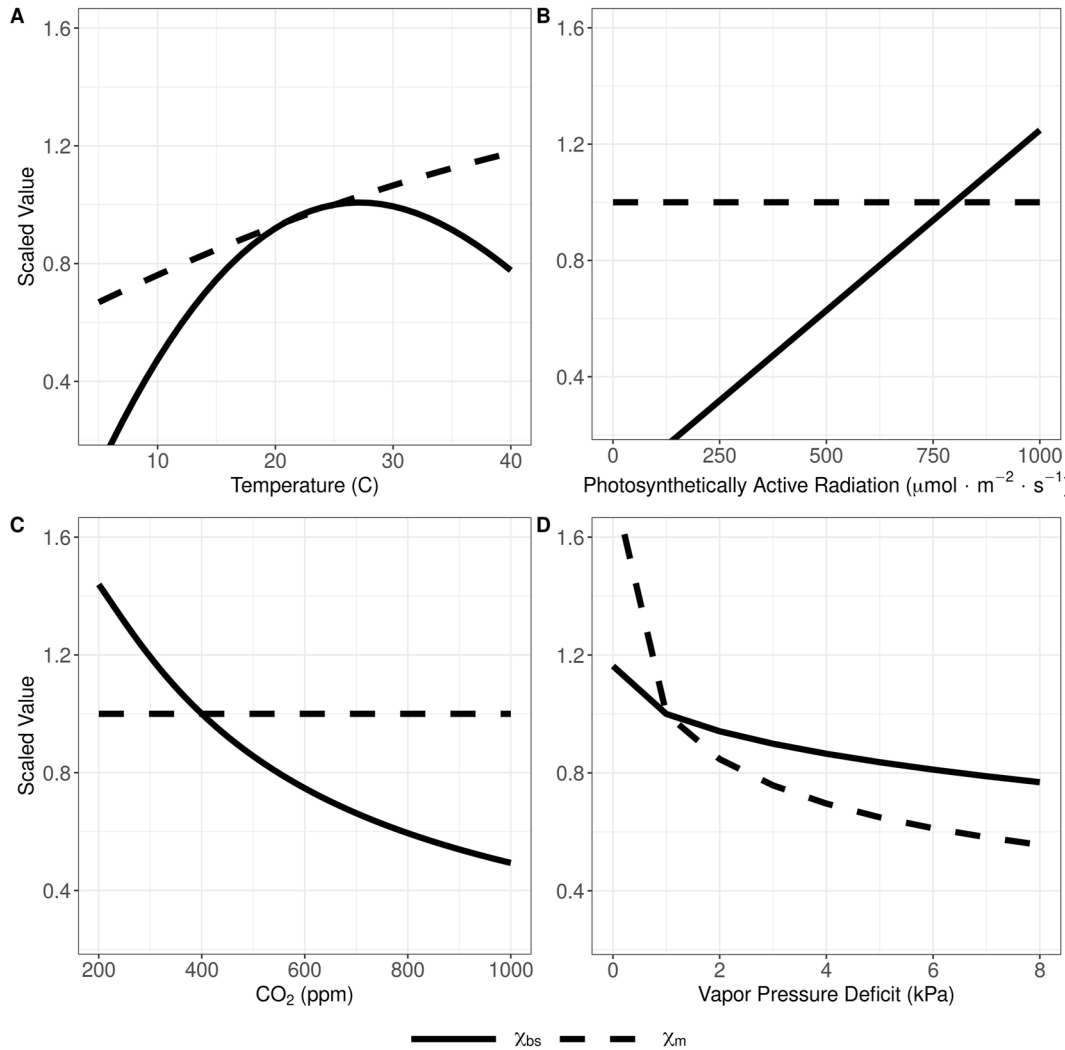

Figure 2. Response of χ_m (dashed black line) and χ_{bs} (solid black line) to (a) temperature, (b) PAR, (c) atmospheric CO_2, and (d) vapor pressure when all others are held constant at standard values. Values are standardized to the predicted value at "standard" conditions (temperature = 25°C, CO_2 = 400 ppm, PAR = 800 μ mol m^{-2} s^{-1} PAR, elevation = 0 m ASL, and VPD = 1 kPa).

$$A_L = A_P = A_C \tag{4}$$

These three rates vary independently from one another based on above-ground environmental conditions, including PAR, temperature, CO_2, and vapor pressure deficit (VPD), allowing us to derive optimally acclimated biochemical rates under different acclimated conditions. To do this, we calculated A_L as in Smith et al. (2019):

$$A_L = \frac{\phi_{PSII} I m \omega^*}{8\theta} \tag{5}$$

where

$$m = \frac{C_i - \Gamma^*}{C_i + 2\Gamma^*} \tag{6}$$

and

$$\omega^* = 1 + \omega - \sqrt{(1+\omega)^2 - 4\theta\omega} \tag{7}$$

and

$$\omega = -(1-2\theta) + \sqrt{(1-\theta)\left(\frac{1}{\frac{4c}{m}\left(1-\theta\frac{4c}{m}\right)} - 4\theta\right)} \tag{8}$$

where I is the incident photosynthetically active photon flux density (μmol $m^{-2}s^{-1}$), θ is the curvature of the PAR response curve, assumed to be 0.85 (unitless), and ϕ_{PSII} is the realized quantum yield of photosynthetic electron transport (mol mol^{-1}). Γ* is the photorespiratory CO_2 compensation point (calculated below in Equation (10)). For the calculation of ω, we assumed the non-varying parameter c, defined as the derivative of A_L with respect to the maximum rate of electron transport (J_{max}), to be equivalent to the standard value for C_3 species, 0.053 (Smith et al., 2019).

There is much uncertainty around the value of ϕ_{PSII}. We expect the value of ϕ_{PSII} to be different for C_4 plants from the value for C_3 plants, and there is evidence that the different sub-types of C_4 may have different ϕ_{PSII} values as well (Ehleringer & Pearcy, 1983; Ogle, 2003). There is experimental evidence that the value of ϕ_{PSII} is lower in C_4 plants (Oberhuber & Edwards, 1993). This is expected because of the additional costs of C_4 photosynthesis, such as the regeneration of PEPc and elevated cyclic transport, which both lower the efficiency of the electron transport system.

Despite these known differences, we have chosen to use the same ϕ_{PSII} value and temperature response equation as is used for C_3 species, which was initially presented in Bernacchi et al. (2001).

$$\phi_{PSII} = -0.080\,5 + 0.022T - 0.00\,034T^2 \tag{9}$$

We chose to use this C_3 specific value because of the lack of consensus for a C_4 value. C_4 specific estimates of ϕ_{PSII} range from 0.45 (Oberhuber & Edwards, 1993) to 0.7 (Farquhar et al., 1989). However, the value used for the intercept term of Equation (9) does not impact the predicted environmental responses only the absolute values of the model predictions. Hence, results of the model presented in this paper are standardized to their values at "standard" conditions (temperature = 25°C, CO_2 = 400 ppm, PAR = 800 μmol m^{-2} s^{-1} PAR, elevation = 0 m ASL, and VPD = 1 kPa) to better compare the trends than absolute values. We discuss the effects of this choice in Section 3.3.

Γ* varies with temperature according to:

$$\Gamma^* = \Gamma^*_{25}\exp\left[\frac{\Delta H_{a(g)}}{R}\left(\frac{1}{298.15} - \frac{1}{T}\right)\right] \tag{10}$$

where Γ^*_{25} is 2.6 Pa at sea level, determined by using the definition $\Gamma^*_{25} = \gamma^* O_m$, where γ^* is half the reciprocal of RuBisCO specificity, 0.000193 (Von Caemmerer, 2000). $\Delta H_{a(g)}$ is 37,830 J mol^{-1}, T is the acclimated leaf temperature in Kelvin, and R is the ideal gas constant (Bernacchi et al., 2001).

A_P is defined in terms of the mesophyll reactions (Von Caemmerer, 2021):

$$A_P = A_{P\text{gross}} - L \tag{11}$$

where $A_{P\text{gross}}$ is the rate of PEP carboxylation and L is the rate of CO_2 leakage from the bundle sheath to the mesophyll. This assumes that the steady state rate of PEP carboxylation and the rate of C_4 acid decarboxylation are equal. $A_{P\text{gross}}$ is the rate of PEP carboxylase, as defined by the Michaleis-Menten equation:

$$A_{P\text{gross}} = \frac{V_{pmax}C_m}{K_p + C_m} \tag{12}$$

where V_{pmax} is the maximum rate of PEPc carboxylation (μmol m^{-2} s^{-1}), K_p is the Michaelis-Menten constant for PEPc (Pa), and C_m is the concentration of CO_2 at the site of carboxylation, the mesophyll chloroplast (Pa).

L, leakage (μmol m^{-2} s^{-1}), is typically given by (Von Caemmerer, 2021):

$$L = g_{bs}\,(C_{bs} - Cm) \tag{13}$$

where C_{bs} and C_m are CO_2 concentrations in μmol m^{-2}, g_{bs} is a constant 3 mmol m^{-2} s^{-1} (Von Caemmerer, 2000).

However, we cannot use this equation, as there are too many unknown variables. Therefore, we rely on the measure of leakiness (ϕ_L), a term coined by Farquhar (1983), which defines leakage as a fraction of the rate of PEP carboxylation and thus describes the efficiency of the C_4 cycle leakiness.

$$\phi_L = L / A_{P\text{gross}} \tag{14}$$

We chose to use a value of 0.2, because values of leakiness inferred from organic material carbon isotope composition varied around 20%–30% (Farquhar, 1983). We left the value of leakiness as a parameter that the user can set for ϕ_L.

This assumption of leakiness allows us to estimate the leakage rate in terms of A_L:

$$L = \frac{\phi_L A_L}{1 - \phi_L} \tag{15}$$

Using Equations (5) and (12), we can solve for optimal V_{pmax} as:

$$V_{pmax} = (A_L + L)(K_p + C_m) C_m \tag{16}$$

K_p is dependent on temperature in the following manner:

$$K_p = K_{p(25)} \exp\left[\Delta H_{a(p)} \frac{T - 298.15}{298.15RT}\right] \tag{17}$$

where $K_{p(25)}$ is equal to 60.5 μmol mol^{-1} and K_p is dependent on temperature in the following manner:

$$K_p = K_{p(25)} \exp\left[\Delta H_{a(p)} \frac{T - 298.15}{298.15RT}\right] \tag{18}$$

where $K_{p(25)}$ is equal to 60.5 μmol mol^{-1} and $\Delta H_{a(p)}$ is equal to 27.2 kJ mol^{-1} (Boyd et al., 2015).

A_C can also be defined using the Michaelis-Menten equation:

$$A_C = \frac{V_{cmax}(C_{bs} - \Gamma^*)}{K_c(1 + O_{bs}/K_o) + C_{bs}} \tag{19}$$

K_c is the Michaelis-Menten coefficient of RuBisCO's carboxylation activity (Pa) and C_{bs} is the concentration of CO_2 at the carboxylation site, the bundle sheath cell (Pa). K_c responds to temperature as follows:

$$K_c = K_{c(25)} \exp\left[\Delta H_{a(c)} \frac{T - 298.15}{298.15RT}\right] \tag{20}$$

where $K_{r(25)}$ is equal to 121 Pa, and $\Delta H_{a(c)}$ is equal to 64.2 kJ mol^{-1} (Boyd et al., 2015).

The Michaelis-Menten coefficient of RuBisCO's oxygenation activity, K_o (Pa) responds to temperature as well.

$$K_o = K_{o(25)} \exp\left[\Delta H_{a(o)} \frac{T - 298.15}{298.15RT}\right] \tag{21}$$

where $K_{o(25)}$ is equal to 29.2 kPa, and $\Delta H_{a(o)}$ is equal to 10.5 kJ mol^{-1} (Boyd et al., 2015).

We can express C_{bs} mathematically as:

$$C_{bs} = C_m + \frac{A_{Pgrsoss} - A_L}{g_{bs}} \tag{22}$$

where C_{bs} and C_m are CO_2 concentrations in μmol m^{-2}, g_{bs} is a constant 3 mmol m^{-2} s^{-1} (Von Caemmerer, 2000).

For direct comparison with trends seen in χ_m, we calculated the ratio of bundle sheath to atmospheric CO_2 as:

$$\chi_{bs} = C_{bs} / C_a \tag{23}$$

We solved for optimal V_{cmax} substituting the A_L from 5 for A_C in 19, yielding:

Table 1
Photosynthetic Parameters (at 25°C) Used in the Model

Parameter	C_4 Value	Unit	Reference	Equation	C_3 value
Θ	0.85	Unitless	Farquhar and Wong (1984)	7 & 8	0.85
c	0.053	Unitless	Smith et al. (2019)	4	0.053
Γ^*_{25}	2.6	Pa	–	10	4.332
$\Delta H_{a(g)}$	37,830	J mol^{-1}	Bernacchi et al. (2001)	10	37,830
$K_{p(25)}$	60.5	μmol mol^{-1}	Boyd et al. (2015)	18	–
$\Delta H_{a(p)}$	27.2	kJ mol^{-1}	Boyd et al. (2015)	18	–
$K_{c(25)}$	121	Pa CO_2	Boyd et al. (2015)	20	41.03
$\Delta H_{a(c)}$	64.2	kJ mol^{-1}	Boyd et al. (2015)	20	79.43
$K_{o(25)}$	29.2	kPa CO_2	Boyd et al. (2015)	21	28.21
$\Delta H_{a(o)}$	10.5	kJ mol^{-1}	Boyd et al. (2015)	21	36.38
g_{bs}	3	mmol m^{-1} s^{-1}	Von Caemmerer (2000)	22	–

Note. The C_3 values are those that were used in the analogous C_3 model (Smith et al., 2019).

$$V_{cmax} = \frac{\phi_{PSII} I m \omega^*}{8\theta} \frac{C_{bs} + K_c (1 + O_{bs}/K_o)}{C_{bs} - \Gamma^*} \tag{24}$$

The optimal maximum rate of electron transport (J_{max}; μmol m^{-2}s^{-1}) is calculated as in Smith et al. (2019) as:

$$J_{\max} = \phi_{PSII} I \omega \tag{25}$$

2.3. Parameterization of the Model

The free parameters in the theoretical model were defined based on empirical data (Table 1). Where possible, these were defined using data from C_4 species.

2.4. C_3 Comparison

We compared simulated photosynthetic rates from the C_4 acclimation model to an analogous C_3 presented in Smith et al. (2019) as updated in Smith and Keenan (2020) (model code available at DOI: 10.5281/zenodo.3874938). Both models rely upon the coordination hypothesis; however, in the C_4 model, there are three possible limiting rates, while the C_3 model has only two (A_P is unique to the C_4 model). While some parameters, such as those for A_L, are identical between the two models, others differ, though they are present in analogous equations. See Table 1 for a full list of parameters with their respective C_3 and C_4 values.

In addition to comparing the absolute values of assimilation rates, we also determined the difference between the rates as a percent of the C_3 level (ΔA):

$$\Delta A = \frac{A_{C_4} - A_{C_3}}{A_{C_3}} * 100 \tag{26}$$

A_{C3} and A_{C4} are the simulated rates of photosynthesis via the C_3 and C_4 pathways respectively. We made these comparisons across multiple CO_2 (200–1,000 ppm), temperature (1–40°C), PAR (0–1,000 μmol m^{-2} s^{-1}), and VPD values (1–8 kPa). In all cases, non-varying conditions were kept constant at standard conditions (CO_2 = 400 ppm, temperature = 25°C, PAR = 800 μmol m^{-2} s^{-1}, and VPD = 1).

2.5. Model Comparison to Global Relative C_4 Abundance

To estimate how well our model predicted the observed patterns of C_4 species abundance, we predicted ΔA values globally and compared these values to relative abundance data from the International Satellite Land-Surface

Climatology Project (Still et al., 2009). The data set estimates the percentage of vegetation (0–100) with the C_4 photosynthetic pathway. The data set is global, divided into 1° grid cells. For the comparison, we selected cells that fell within grasslands, open shrublands, savannas, and woody savannas, as defined by the MODIS Land Cover Type Product MCD12Q1 International Geosphere-Biosphere Programme (IGBP) legend and class descriptions (Friedl & Sulla-Menashe, 2015). These land cover types were selected because they each had high values of C_4 dominance. We fit a linear regression with ΔA as the dependent variable and the percentage of C_4 vegetation as the independent variable. We calculated Pearson's correlation coefficient to assess the strength of the relationship between our predicted ΔA value and the C_4 percent coverage.

2.6. Instantaneous Model

To compare the acclimated response to the unacclimated instantaneous response, we developed a second model without acclimation. This instantaneous model used the same parameters and core equations, but with static values for χ_m, χ_{bs}, J_{max}, V_{pmax}, and V_{cmax}. The values used were those predicted from the acclimated model under standard conditions (temperature = 25°C, CO_2 = 400 ppm, PAR = 800 μmol m^{-2} s^{-1}, elevation = 0 m ASL, and VPD = 1 kPa). We compared acclimated and unacclimated photosynthetic rates across a range of CO_2 (200–1,000 ppm), temperature (1–40°C), PAR (0–1,000 μmol m^{-2} s^{-1}), and VPD_0 values (0–8 kPa). In all cases, non-varying conditions were kept constant at the standard conditions listed above.

3. Results

3.1. Optimal Photosynthesis-Environment Responses

In response to increased temperature, our theory predicted an increase in χ_m (Figure 2). Two factors contributed to the increase: an increase in the Michaelis-Menten constant of PEPc (K_p) and a decrease in the viscosity of water (Equation 2). Increased VPD resulted in a non-linear decrease in χ_m directly due to D's presence in Equation (2). Changes in CO_2 and PAR did not impact χ_m, as these conditions are not part of the theoretical equation (Equation 2). This represents the assumption that no photorespiration is occurring, and is a key difference between the C_3 and C_4 model.

The χ_{bs} value follows the same trends as χ_m (Figure 2).

Predicted optimal J_{max} increases with temperature, PAR, and CO_2, and decreases slightly with VPD (Figure 3). The non-linear increase with temperature is due to the simultaneous increase of ϕ_{PSII} and Γ* (within the ω term), which control J_{max} values linearly in Equation (25). The linear increase with PAR is predicted in Equation (25). Unlike the other biochemical processes, J_{max} increases very slightly with CO_2. Finally, J_{max} decreases with VPD due to decreases in C_m within the ω term (Equations 6 and 8).

The model predicts an increase in V_{pmax} with temperature and PAR (Figure 3). As noted in Equation (18), the Michaelis-Menten constant, K_p is temperature dependent, as is ϕ_{PSII} (Equation 9). As both are present in the numerator of Equation (16), V_{pmax} increases with temperature. V_{pmax} increased linearly in response to PAR, as a result of a linear increase in A_L. V_{pmax} decreased in response to increasing CO_2 levels, as more CO_2 allowed for nutrient-use of PEP carboxylation necessary to equate A_L and A_p. The model predicted a slight, non-linear, increase in V_{pmax} with increased vapor pressure deficit due to reduced χ_m.

Like V_{pmax}, the optimal V_{cmax} increases with temperature and PAR and decreases with CO_2 due to similar drivers (Figure 3). The temperature increases continuously within the physiologically relevant range, rather than peaking before 40°C due to the combined effects increases in K_c and Γ* (Equation 24). V_{cmax} increases with PAR linearly. The linear relationship is due to the dependence of χ_{bs} on PAR (Equation 22) in addition to the linear relationship of A_L with PAR (Equation 24). The decrease of V_{cmax} in response to increased CO_2 is due to a down-regulation of carboxylation activity to match A_C rates to the unaffected A_L rates. V_{cmax} decreases to a lesser degree than V_{pmax} with increasing CO_2 due to the greater partial pressure of CO_2 in the bundle sheath as compared to the mesophyll. V_{cmax} increased slightly in response to VPD.

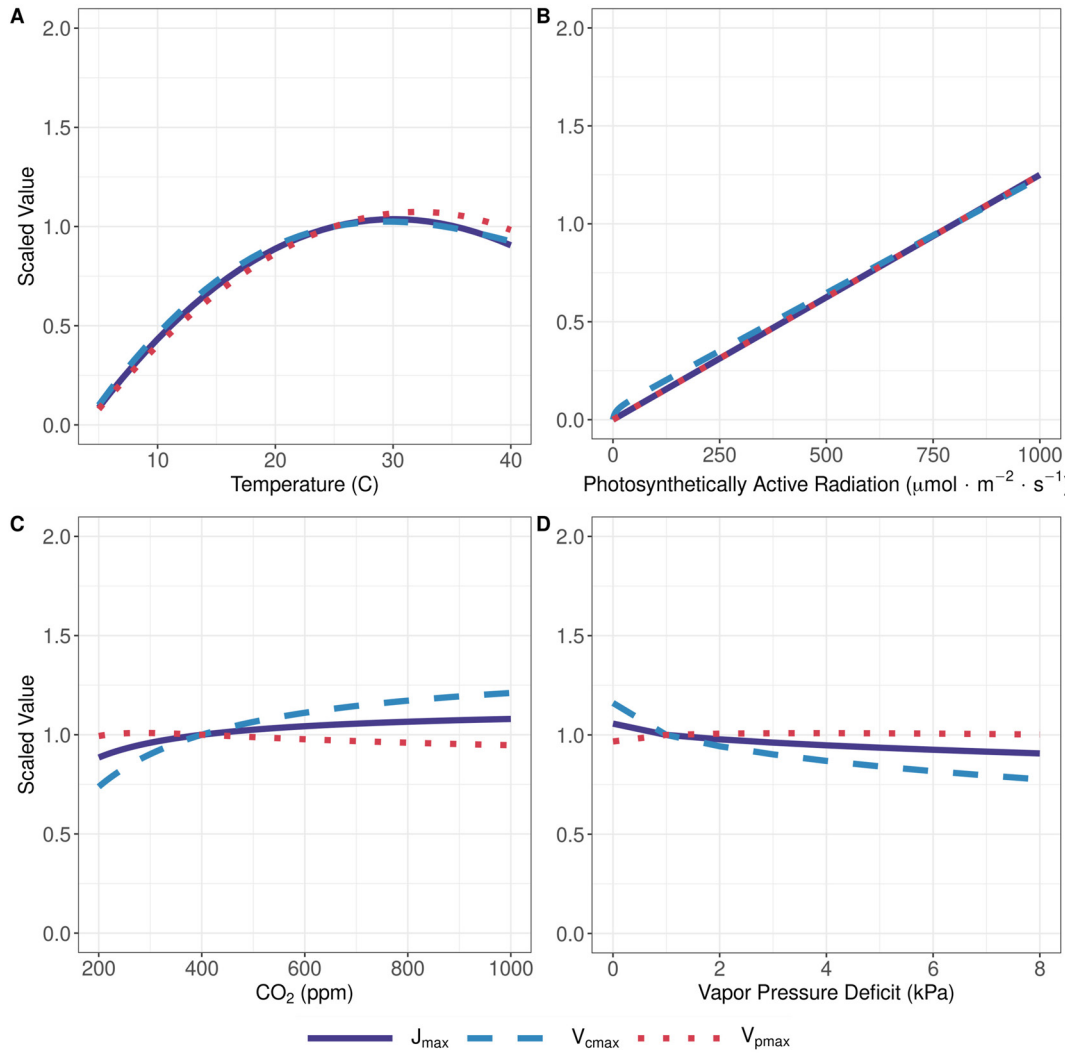

Figure 3. Response of optimal J_{max} (solid purple line), V_{cmax} (dashed blue line), and V_{pmax} (dotted red line) to (a) temperature, (b) PAR, (c) atmospheric CO_2, and (d) vapor pressure when all others are held constant at standard values. Values are standardized to the predicted value at "standard" conditions (temperature = 25°C, CO_2 = 400 ppm, PAR = 800 μmol m^{-2} s^{-1}, elevation = 0 m ASL, and VPD = 1 kPa). At standard conditions, J_{max} is equal to 457.75, V_{cmax} is equal to 77.62, and V_{pmax} is equal to 53.96.

3.2. Allocation of Resources to Different Biochemical Processes

Figure 4 shows the ratios of J_{max} to V_{cmax}, J_{max} to V_{pmax}, and V_{cmax} to V_{pmax} across varying temperature and PAR values. There is no change in ratios in response to PAR, as all of the biochemical variables respond linearly to PAR. However, the ratios all do vary, if only slightly in response to temperature, CO_2 and VPD. J_{max}: V_{cmax} decreases with temperature, as the increase of the V_{cmax} with temperature quickly outpaces the increase of J_{max}. J_{max}: V_{pmax} decreased slightly across the temperature range. This muted response is due to J_{max} and V_{pmax}'s similar responses as seen in Figure 3. The V_{cmax} to V_{pmax} ratio increases with temperature. The increase of V_{cmax}:V_{pmax} with temperature is due to V_{cmax}'s large absolute values due to the carbon concentrating mechanism, and V_{cmax}'s increase with temperature. None of the ratios changed significantly with PAR or VPD.

3.3. Predicted Optimal Photosynthetic Rates

First we look at the general trends of acclimated C_4 photosynthesis over environmental conditions (Figure 5). Predicted optimal *A* increased non-linearly with temperature to approximately 25°C after which it decreased.

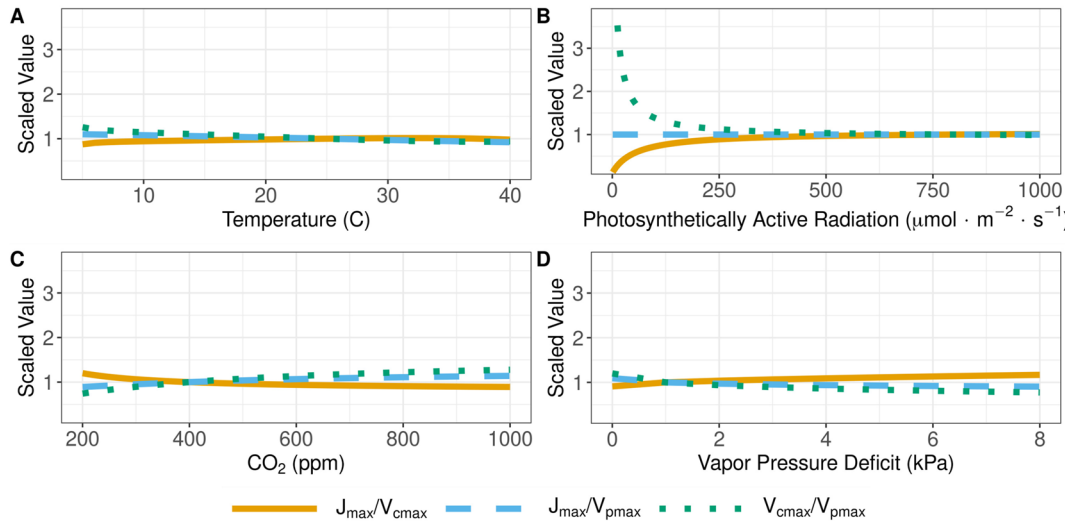

Figure 4. Predicted response of optimal ratios of J_{max}:V_{cmax} (solid yellow line), J_{max}:V_{pmax} (dashed blue line), and V_{cmax}:V_{pmax} (dotted green line) to (a) temperature and (b) PAR when all other conditions are held constant at standard values. Values are standardized to the predicted value at "standard" conditions (temperature = 25°C, CO_2 = 400 ppm, PAR = 800 μmol m^{-2} s^{-1}, elevation = 0 m ASL, and VPD = 1 kPa). At standard conditions, J_{max}:V_{cmax} is equal to 5.90, J_{max}:V_{pmax} is equal to 8.48, and V_{cmax}:V_{pmax} is equal to 1.44.

A increased linearly with PAR, concurrent with increases in biochemical process rates. *A* increases with atmospheric CO_2 and decreases with VPD.

When the absolute values of assimilation rates are compared, C_4 photosynthetic rates were always higher than the C_3 rates (Figure 5). This is possibly due to the model overestimation of C_4 photosynthesis because of the use of an overestimated ϕ_{PSII} value (as discussed in Equation (9)). With the given ϕ_{PSII} value, photosynthetic rates were most similar at low light, low temperature, and high CO_2 levels.

3.4. Acclimated Versus Non-Acclimated Responses

Optimal photosynthetic acclimation either increased assimilation or decreased photosynthetic costs (Figure 5). For all environmental conditions, when the environmental variables are equal to the acclimated conditions, the assimilation rates in the acclimated and instantaneous models are equal. For temperatures above or below the acclimation temperature, the assimilation was higher for the acclimated model. With increasing PAR, instantaneous assimilation is unable to increase beyond the acclimated condition and plateaus, whereas the acclimation model continues to increase linearly. Similarly, with increasing CO_2 the rate of increase of assimilation slows below the acclimated value of CO_2. However, acclimation results in decreased assimilation with increasing VPD. The instantaneous model is unresponsive to VPD because χ_m is not decreasing. We expected acclimated plants to decrease assimilation with increasing VPD to conserve water, therefore minimizing the cost of assimilation.

3.5. Model-Data Comparison

Global values for ΔA correlated strongly with the percent of vegetation with the C_4 photosynthetic pathway from the International Satellite Land-Surface Climatology Project (Still et al., 2009; $P < 0.001$; Figure 6). This indicates that our model captures trends in the distribution of plants with different photosynthetic types globally.

4. Discussion

The C_4 photosynthetic pathway accounts for 20% of global carbon assimilation and is present in many critical agricultural species, including maize (Ehleringer et al., 1997). While C_4 species are known to acclimate to changes in environmental conditions (Sage & McKown, 2006), ESMs do not include this acclimation. Here, we present a novel theoretical model for C_4 photosynthetic acclimation suitable for use in ESMs. In addition to its

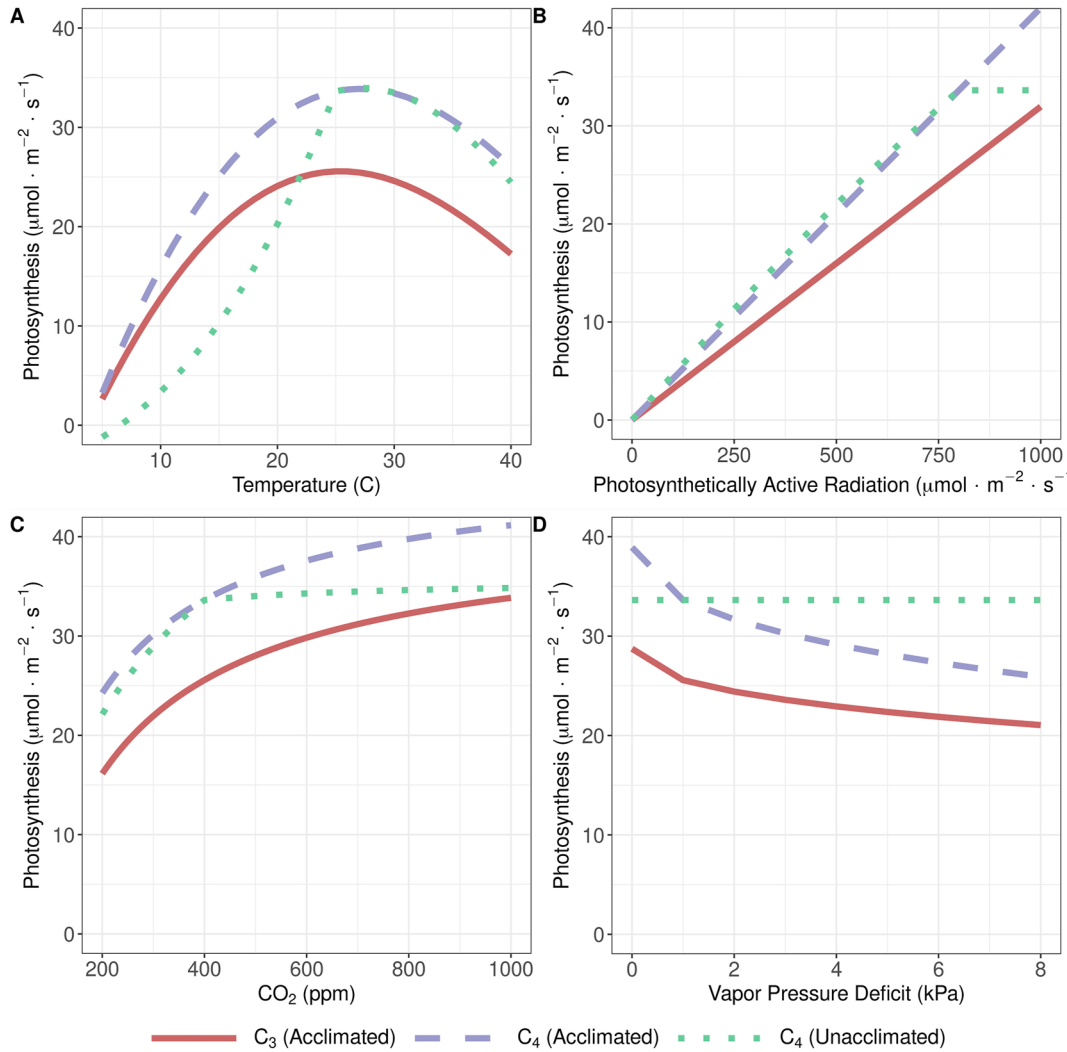

Figure 5. Predicted photosynthetic assimilation by acclimated C_4 plants (dashed purple line), unacclimated C_4 plants (dotted green line) and acclimated C_3 plants (solid red line) varies with (a) temperature, (b) PAR, (c) atmospheric CO_2, and (d) vapor pressure deficit when all other conditions are held constant at standard values (temperature = 25°C, CO_2 = 400 ppm, PAR = 800 μmol m^{-2} s^{-1}, elevation = 0 m ASL, and VPD = 1 kPa). C_4 rates were predicted from the model presented in the text, while C_3 rates were predicted from (Smith et al., 2019) as updated in Smith and Keenan (2020) (DOI: 10.5281/zenodo.3874938). In both cases, similar ϕ_{PSII} values were used. At standard conditions, the C_4 model predicts photosynthesis rates of 33.63 μmol m^{-2} s^{-1}.

potential to improve ESM simulations' reliability, the theoretical model may also be informative for understanding other ecological aspects of C_4 species, including their competition with C_3 species under different environmental contexts. Below we discuss the insights we gleaned from this model exercise and its potential for improving our understanding of plant ecology under variable environments.

4.1. Insights Into Photosynthetic Efficiency and Plasticity

Our theory provides insights into long-appreciated aspects of C_4 photosynthesis, including the mechanisms underlying their water and nutrient-use efficiencies and photosynthetic acclimation. First, our theory's broad fidelity to global observation-based estimates of C_4 species abundance suggests that, across large spatial scales, realized assimilation are principally determined by the optimization in response to environmental conditions. It is essential to note that photosynthetic data for C_4 plants is more scarce than data available for C_3 plants (Kattge & Sandel, 2020), limiting our ability to more directly test the model's mechanisms. Nonetheless, our theory provides

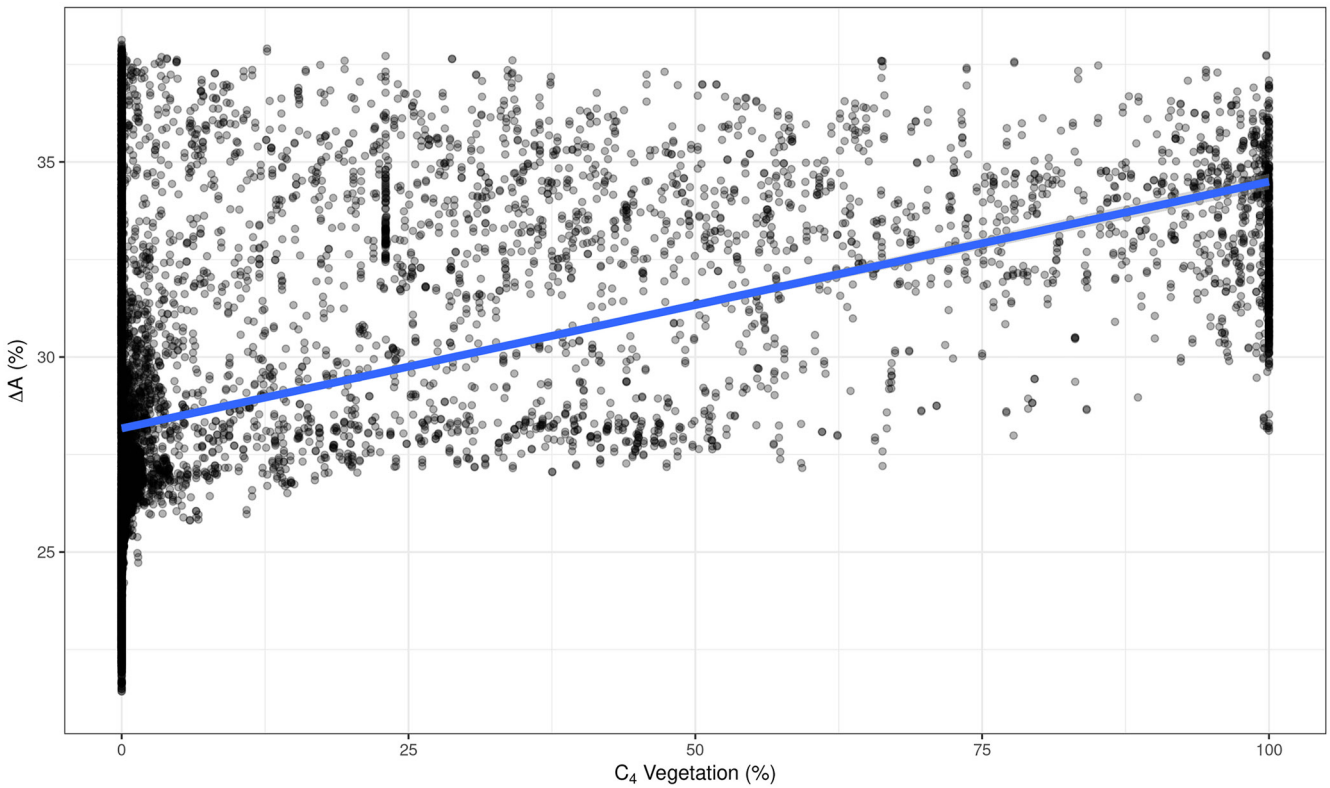

Figure 6. Relationship between the predicted optimal photosynthetic advantage of C_4 over C_3 plants (ΔA) to the percentage of C_4 vegetation from the International Satellite Land-Surface Climatology Project (Still et al., 2009). Points represent 1° grid cells in locations described by MODIS as grasslands, open shrublands, savannas, or woody savannas. Insert statistics show the statistics from a linear model relationship of ΔA and percent C_4 vegetation. The blue line show the fit from the linear model.

a framework for developing hypotheses for how C_4 photosynthesis varies across environments. It will be critical to explore these responses across a range of temporal scales as more data becomes available.

Second, Equation (2) predicts χ_m to be 0.56 under "standard" conditions (temperature = 25°C, CO_2 = 400 ppm, PAR = 800 μmol m^{-2} s^{-1}, elevation = 0 m ASL, and VPD = 1 kPa). This χ value is considerably lower than values found in C_3 plants (Wang et al., 2017), indicating higher WUE in C_4 plants than C_3 plants. Our theory confirms that this observed difference between photosynthetic types is due to the relative lack of oxygenation in C_4 plants (Sage, 1999; Sage & McKown, 2006).

Third, the increased concentrations of CO_2 at the site of RuBisCO fixation (C_{bs}) relative to that in C_3 plants allows for a reduced need for RuBisCO enzymes, thus leading to potentially greater NUE in C_4 plants. Greater NUE in C_4 versus C_3 has been observed previously (Sage & Pearcy, 1987). Our theory confirms previous estimates indicating that this is due to RuBisCO's greater efficiency due to reduced oxygenation and further reinforces the importance of high C_{bs} in driving this response (Sage et al., 1987).

Finally, our theory sheds light on the photosynthetic plasticity observed in C_4 plants. Experimental studies have shown that C_4 photosynthesis is less sensitive than C_3 photosynthesis in general (Sage & McKown, 2006) and in response to CO_2 (Ainsworth & Long, 2005) and VPD (Wherley & Sinclair, 2009) in particular. The CO_2 and VPD responses are consistent with our theory. Importantly, our theory confirms that this is due to greater efficiency afforded to C_4 species by concentrating a high amount of CO_2 in the bundle sheath. Notably, our theory also finds high plasticity in response to temperature and PAR, similar to that of C_3 species, suggesting that the mechanisms driving acclimation to these conditions (Smith et al., 2019; Smith & Keenan, 2020; Wang et al., 2017) are similar across species with different photosynthetic types, confirming previous experimental results in response to temperature (Smith & Dukes, 2017; Yamori et al., 2014). However, previous experimental results suggest the PAR response of C_4 species to be less plastic than C_3 species (Sage & McKown, 2006), contrasting with

our results. Coupled theory-experiment analyses would help to understand further the mechanisms driving this disconnect.

As discussed with Equation (2), we are uncertain in the absolute values of the model predictions due to uncertainties around key parameters. However, we did compare the model predictions with experimental data and existing theoretical predictions.

When compared with the experimental data from Massad et al. (2007) and the theoretical predictions from (D. Chen et al., 1994), our model predictions for photosynthetic rate, J_{max}, and V_{cmax}, were all high but relatively close. Our predictions for V_{pmax}, however, were very low. Our predictions at a temperature of 25°C was closest to V_{pmax} measurements at much lower temperatures. These discrepancies could be due to the existing work's focus on instantaneous responses rather than acclimation, or due to inaccuracies in the derivation or parameterization of the model. We believe that a better parameterization of values such as ϕ_{PSII} would lead to a better approximation of the data.

4.2. Acclimation to Elevated Temperature and CO_2 Reduces Optimal Enzyme Requirements, Possibly Reducing Nitrogen Use

These results suggest that future, warmer conditions may increase the photosynthetic rates of C_4 plants (Figure 5). However, our theory suggests that this will come alongside a reduction in nitrogen-heavy carboxylation enzymes, possibly increasing future nutrient-use efficiency (NUE), as has been suggested for C_3 plants (Smith & Keenan, 2020).

The potential reduction in leaf-level nitrogen demand suggested by our theory may critically impact ESM simulations that include a dynamic N cycle. Such models indicate that progressive nitrogen limitation will limit increases in future productivity driven by increases in atmospheric CO_2 (Finzi et al., 2007; Luo et al., 2004; P. Reich et al., 2006; Thornton et al., 2007b; Wieder et al., 2015; Zhu et al., 2019). To correctly predict the magnitude and extent of progressive nitrogen limitation, models of photosynthesis must correctly simulate changing leaf NUE. Our theory predicts increased NUE in the future, driven by a critical tenant of the least-cost hypothesis: maximizing photosynthesis while minimizing carbon costs (Wright et al., 2003). Acclimation led to increased NUE in C_3 plants in models (Smith & Keenan, 2020), and in the field (Davey et al., 1999). Long-term field experiments with C_4 plants observed increased NUE in response to warming and elevated CO_2 (Carvalho et al., 2020). These results suggest that future increases in leaf NUE must be considered by ESMs to predict future ecosystem N limitation accurately. Our model provides an avenue for doing this for C_4 plants.

4.3. C_4 Advantage Will Decrease in Future

Our theory indicates that future high temperature, high CO_2 environments will disproportionately favor C_3 plants over C_4 plants. While we expected C_3 photosynthetic rates to increase with temperature and CO_2 (Smith & Dukes, 2013), we expected C_4 plants to increase with temperature only (Alberto et al., 1996), while remaining unchanged or to increase very little in response to CO_2 (Poorter & Navas, 2003; Sage & Coleman, 2001). Our model predicted these results when compared to the analogous C_3 model (Smith et al., 2019). We found that the ΔA value increased with temperature and decreased with CO_2. When the two vary simultaneously, C_4 retain their current competitive advantage in high CO_2 environments only when the acclimated temperature is also very high. For example, at a growing season temperature of 15°C at 400 ppm CO_2, C_4 photosynthesis assimilates roughly 26% more carbon than C_3 photosynthesis. However, this same ΔA value can only be achieved at a growing season temperature of 37°C when CO_2 reaches 1,000 ppm. Looking forward, these comparisons may indicate future restrictions of C_4 species to extremely hot environments. A similar comparison between ΔA values at current (400 ppm) and low (250 ppm) CO_2 values can also be used to infer the evolutionary history of C_4 plants, many of which first appeared when CO_2 levels were much lower than they are today.

Previous results question the longevity of such a competitive decline of C_4 plants when plants acclimate to increased CO_2 levels on a multi-decadal timescale (P. B. Reich et al., 2018). That study and others (Wolf & Ziska, 2018) indicate the importance of including nutrient feedbacks, plant growth rates, and plant life spans in systems where nutrients or water may be limiting. The ability of C_4 plants to accumulate organic matter in the soil may further help C_4 plants to thrive in nutrient and water poor environment, and may help to ameliorate the

ΔA differential caused by high CO_2 concentrations, keeping C_4 plants competitive in a greater number of habitats. Coupling our theory to a model that can predict these higher-order processes is the next step in understanding the interplay between leaf photosynthesis and ecosystem-scale processes.

4.4. Future Work

We hope that future work in the field will address the relative lack of experiments with C_4 plants compared to C_3 plants. We were limited in the construction of this model by the relative lack of C_4-specific experimental data. More experimental data is needed to find C_4-specific values for parameters such as ϕ_{PSII} that are incorrectly assumed to be equal to C_3 values here. Other experiments designed to measure longer-term acclimation could be used to test and validate these model predictions.

This study provides the basis for the incorporation of C_4 photosynthetic acclimation into ESMs. Some work has been done to incorporate C_3 photosynthetic acclimation into ESMs (Smith & Dukes, 2013), but little work has been done to incorporate C_4 photosynthetic acclimation. The model presented here provides the means to calculate acclimated rates of χ_m, χ_{bs}, J_{max}, V_{pmax}, and V_{cmax}. In an ESM, these rates could be calculated using acclimated conditions and used as reference rates that are modified based on instantaneous conditions. One major difficulty is determining the appropriate timescale for acclimation, which is unknown and can impact model simulations (Dietze, 2014). To more reliably simulate acclimated processes, future work should focus on determining this time scale and the drivers of its variability.

Data Availability Statement

Data used from Cornwell et al. (2018) was retrieved from https://github.com/wcornwell/leaf13C. All data, model code, and analysis code, including the code to reproduce the figures have been published in an open-access repository (DOI: 10.5281/zenodo.5239881).

Acknowledgments
We acknowledge support from the National Science Foundation (DEB-2045968) and Texas Tech University. This work is a contribution to the LEMONTREE (Land Ecosystem Models based On New Theory, obseRvations and ExperimEnts) project, funded through the generosity of Eric and Wendy Schmidt by recommendation of the Schmidt Futures program. We thank two anonymous reviewers for their helpful comments on earlier drafts of the manuscript.

References

Ainsworth, E. A., & Long, S. P. (2005). What have we learned from 15 years of free-air CO_2 enrichment (face)? A meta-analytic review of the responses of photosynthesis, canopy properties and plant production to rising CO_2. *New Phytologist*, *165*(2), 351–372. https://doi.org/10.1111/j.1469-8137.2004.01224.x

Alberto, A., Ziska, L., Cervancia, C., & Manalo, P. (1996). The influence of increasing carbon dioxide and temperature on competitive interactions between a C_3 crop, rice (oryza sativa) and a c4 weed (*Echinochloa glabrescens*). *Functional Plant Biology*, *23*, 795–802. https://doi.org/10.1071/pp9960795

Bazzaz, F. A. (1990). The response of natural ecosystems to the rising global CO_2 levels. *Annual Review of Ecology and Systematics*, *21*(1), 167–196. https://doi.org/10.1146/annurev.es.21.110190.001123

Bellasio, C., & Griffiths, H. (2014). Acclimation to low light by C_4 maize: Implications for bundle sheath leakiness. *Plant, Cell and Environment*, *37*(5), 1046–1058. https://doi.org/10.1111/pce.12194

Bernacchi, C., Singsaas, E., Pimentel, C., Portis, A., Jr, & Long, S. (2001). Improved temperature response functions for models of rubisco-limited photosynthesis. *Plant, Cell and Environment*, *24*(2), 253–259. https://doi.org/10.1111/j.1365-3040.2001.00668.x

Berry, J., & Bjorkman, O. (1980). Photosynthetic response and adaptation to temperature in higher plants. *Annual Review of Plant Physiology*, *31*(1), 491–543. https://doi.org/10.1146/annurev.pp.31.060180.002423

Boardman, N. T. (1977). Comparative photosynthesis of sun and shade plants. *Annual Review of Plant Physiology*, *28*(1), 355–377. https://doi.org/10.1146/annurev.pp.28.060177.002035

Booth, B. B., Jones, C. D., Collins, M., Totterdell, I. J., Cox, P. M., Sitch, S., et al. (2012). High sensitivity of future global warming to land carbon cycle processes. *Environmental Research Letters*, *7*(2), 024002. https://doi.org/10.1088/1748-9326/7/2/024002

Boyd, R. A., Gandin, A., & Cousins, A. B. (2015). Temperature responses of C_4 photosynthesis: Biochemical analysis of rubisco, phosphoenolpyruvate carboxylase, and carbonic anhydrase in *Setaria viridis*. *Plant Physiology*, *169*(3), 1850–1861.

Carvalho, J., Ferreira Barreto, R., Prado, R., Habermann, E., Branco, R., & Martinez, C. (2020). Elevated CO_2 and warming change the nutrient status and use efficiency of *Panicum maximum* jacq. *PLoS One*, *15*, e0223937. https://doi.org/10.1371/journal.pone.0223937

Chen, D., Coughenour, M., Knapp, A., & Owensby, C. (1994). Mathematical simulation of C_4 grass photosynthesis in ambient and elevated CO_2. *Ecological Modelling*, *73*(1–2), 63–80. https://doi.org/10.1016/0304-3800(94)90098-1

Chen, J.-L., Reynolds, J. F., Harley, P. C., & Tenhunen, J. D. (1993). Coordination theory of leaf nitrogen distribution in a canopy. *Oecologia*, *93*(1), 63–69. https://doi.org/10.1007/bf00321192

Collatz, G. J., Ball, J. T., Grivet, C., & Berry, J. A. (1991). Physiological and environmental regulation of stomatal conductance, photosynthesis and transpiration: A model that includes a laminar boundary layer. *Agricultural and Forest Meteorology*, *54*(2–4), 107–136. https://doi.org/10.1016/0168-1923(91)90002-8

Collatz, G. J., Ribas-Carbo, M., & Berry, J. (1992). Coupled photosynthesis-stomatal conductance model for leaves of C_4 plants. *Functional Plant Biology*, *19*(5), 519–538. https://doi.org/10.1071/pp9920519

Cornwell, W. K., Wright, I. J., Turner, J., Maire, V., Barbour, M. M., Cernusak, L. A., et al. (2018). Climate and soils together regulate photosynthetic carbon isotope discrimination within C_3 plants worldwide. *Global Ecology and Biogeography*, *27*(9), 1056–1067. https://doi.org/10.1111/geb.12764

Davey, P., Parsons, A., Atkinson, L., Wadge, K., & Long, S. P. (1999). Does photosynthetic acclimation to elevated CO_2 increase photosynthetic nitrogen-use efficiency? A study of three native UK grassland species in open-top chambers. *Functional Ecology*, *13*, 21–28. https://doi.org/10.1046/j.1365-2435.1999.00004.x

Dietze, M. C. (2014). Gaps in knowledge and data driving uncertainty in models of photosynthesis. *Photosynthesis Research*, *119*(1), 3–14. https://doi.org/10.1007/s11120-013-9836-z

Dusenge, M. E., Duarte, A. G., & Way, D. A. (2019). Plant carbon metabolism and climate change: Elevated CO_2 and temperature impacts on photosynthesis, photorespiration and respiration. *New Phytologist*, *221*(1), 32–49. https://doi.org/10.1111/nph.15283

Dwyer, S. A., Ghannoum, O., Nicotra, A., & Von Caemmerer, S. (2007). High temperature acclimation of C_4 photosynthesis is linked to changes in photosynthetic biochemistry. *Plant, Cell and Environment*, *30*(1), 53–66. https://doi.org/10.1111/j.1365-3040.2006.01605.x

Ehleringer, J., Cerling, T., & Helliker, B. (1997). C-4 photosynthesis, atmospheric CO_2 and climate. *Oecologia*, *10112*, 285–299. https://doi.org/10.1007/s004420050311

Ehleringer, J., & Pearcy, R. W. (1983). Variation in quantum yield for CO_2 uptake among C_3 and C_4 plants. *Plant Physiology*, *73*(3), 555–559. https://doi.org/10.1104/pp.73.3.555

Farquhar, G. D. (1983). On the nature of carbon isotope discrimination in C_4 species. *Functional Plant Biology*, *10*(2), 205–226. https://doi.org/10.1071/pp9830205

Farquhar, G. D., Ehleringer, J., & Hubick, K. (1989). Carbon isotope discrimination and photosynthesis. *Annual Review of Plant Physiology*, *40*. https://doi.org/10.1146/annurev.pp.40.060189.002443

Farquhar, G. D., von Caemmerer, S. v., & Berry, J. A. (1980). A biochemical model of photosynthetic CO_2 assimilation in leaves of C_3 species. *Planta*, *149*(1), 78–90. https://doi.org/10.1007/bf00386231

Farquhar, G. D., & Wong, S. C. (1984). An empirical model of stomatal conductance. *Functional Plant Biology*, *11*(3), 191–210. https://doi.org/10.1071/pp9840191

Finzi, A. C., Norby, R. J., Calfapietra, C., Gallet-Budynek, A., Gielen, B., Holmes, W. E., et al. (2007). Increases in nitrogen uptake rather than nitrogen-use efficiency support higher rates of temperate forest productivity under elevated co2. *Proceedings of the National Academy of Sciences*, *104*(35), 14014–14019. https://doi.org/10.1073/pnas.0706518104

Friedl, M., & Sulla-Menashe, D. (2015). Mcd12q1 modis/terra+aqua land cover type yearly l3 global 500 m SIN grid v006. *NASA EOSDIS Land Processes DAAC*. https://doi.org/10.5067/MODIS/MCD12Q1.006

Friend, A. D. (2010). Terrestrial plant production and climate change. *Journal of Experimental Botany*, *61*(5), 1293–1309. https://doi.org/10.1093/jxb/erq019

Kanai, R., & Edwards, G. E. (1999). The biochemistry of C4 photosynthesis. *C4 Plant Biology*, *49*, 87.

Kattge, J., & Knorr, W. (2007). Temperature acclimation in a biochemical model of photosynthesis: A reanalysis of data from 36 species. *Plant, Cell and Environment*, *30*(9), 1176–1190. https://doi.org/10.1111/j.1365-3040.2007.01690.x

Kattge, J., & Sandel, B. (2020). TRY plant trait database-enhanced coverage and open access. *Global Change Biology*, *26*(9), 5343.

King, A. W., Gunderson, C. A., Post, W. M., Weston, D. J., & Wullschleger, S. D. (2006). Plant respiration in a warmer world. *Science*, *312*(5773), 536–537. https://doi.org/10.1126/science.1114166

Lombardozzi, D. L., Bonan, G. B., Smith, N. G., Dukes, J. S., & Fisher, R. A. (2015). Temperature acclimation of photosynthesis and respiration: A key uncertainty in the carbon cycle-climate feedback. *Geophysical Research Letters*, *42*(20), 8624–8631. https://doi.org/10.1002/2015gl065934

Luo, Y., Su, B., Currie, W. S., Dukes, J. S., Finzi, A., Hartwig, U., et al. (2004). Progressive nitrogen limitation of ecosystem responses to rising atmospheric carbon dioxide. *BioScience*, *54*(8), 731–739. https://doi.org/10.1641/0006-3568(2004)054[0731:pnloer]2.0.co;2

Maherali, H., Reid, C., Polley, H., Johnson, H., & Jackson, R. (2002). Stomatal acclimation over a subambient to elevated CO_2 gradient in a C_3/C_4 grassland. *Plant, Cell and Environment*, *25*(4), 557–566. https://doi.org/10.1046/j.1365-3040.2002.00832.x

Maire, V., Martre, P., Kattge, J., Gastal, F., Esser, G., Fontaine, S., & Soussana, J.-F. (2012). The coordination of leaf photosynthesis links c and n fluxes in C_3 plant species. *PLoS One*, *7*(6), e38345. https://doi.org/10.1371/journal.pone.0038345

Massad, R.-S., Tuzet, A., & Bethenod, O. (2007). The effect of temperature on C_4-type leaf photosynthesis parameters. *Plant, Cell and Environment*, *30*(9), 1191–1204. https://doi.org/10.1111/j.1365-3040.2007.01691.x

Mercado, L. M., Medlyn, B. E., Huntingford, C., Oliver, R. J., Clark, D. B., Sitch, S., et al. (2018). Large sensitivity in land carbon storage due to geographical and temporal variation in the thermal response of photosynthetic capacity. *New Phytologist*, *218*(4), 1462–1477. https://doi.org/10.1111/nph.15100

Oberhuber, W., & Edwards, G. E. (1993). Temperature dependence of the linkage of quantum yield of photosystem II to CO_2 fixation in C_4 and C_3 plants. *Plant Physiology*, *101*(2), 507–512. https://doi.org/10.1104/pp.101.2.507

Ogle, K. (2003). Implications of interveinal distance for quantum yield in C_4 grasses: A modeling and meta-analysis. *Oecologia*, *136*(4), 532–542. https://doi.org/10.1007/s00442-003-1308-2

Poorter, H., & Navas, M.-L. (2003). Plant growth and competition at elevated CO_2: On winners, losers and functional groups: Tansley review. *New Phytologist*, *157*, 175–198. https://doi.org/10.1046/j.1469-8137.2003.00680.x

Prentice, I. C., Dong, N., Gleason, S. M., Maire, V., & Wright, I. J. (2014). Balancing the costs of carbon gain and water transport: Testing a new theoretical framework for plant functional ecology. *Ecology Letters*, *17*(1), 82–91. https://doi.org/10.1111/ele.12211

Reich, P., Hobbie, S., Lee, T., Ellsworth, D., West, J., Tilman, D., et al. (2006). Nitrogen limitation constrains sustainability of ecosystem response to CO_2. *Nature*, *440*, 922–925. https://doi.org/10.1038/nature04486

Reich, P. B., Hobbie, S. E., Lee, T. D., & Pastore, M. A. (2018). Unexpected reversal of C_3 versus C_4 grass response to elevated CO_2 during a 20-year field experiment. *Science*, *360*(6386), 317–320. https://doi.org/10.1126/science.aas9313

Sage, R. F. (1999). Why C4 photosynthesis. *C4 Plant Biology*, *3–16*.

Sage, R. F., & Coleman, J. (2001). Effects of low atmospheric CO_2 on plants: More than a thing of the past. *Trends in Plant Science*, *6*, 1360–1385. https://doi.org/10.1016/s1360-1385(00)01813-6

Sage, R. F., & Kubien, D. (2007). The temperature response of C_3 and C_4 photosynthesis. *Plant, Cell and Environment*, *30*(9), 1086–1106. https://doi.org/10.1111/j.1365-3040.2007.01682.x

Sage, R. F., & McKown, A. D. (2006). Is C_4 photosynthesis less phenotypically plastic than C_3 photosynthesis? *Journal of Experimental Botany*, *57*(2), 303–317. https://doi.org/10.1093/jxb/erj040

Sage, R. F., & Pearcy, R. W. (1987). The nitrogen use efficiency of C_3 and C_4 plants. *Plant Physiology*, *84*(3), 959–963. https://doi.org/10.1104/pp.84.3.959

Sage, R. F., Pearcy, R. W., & Seemann, J. R. (1987). The nitrogen use efficiency of C_3 and C_4 plants. *Plant Physiology*, *85*(2), 355–359. https://doi.org/10.1104/pp.85.2.355

Smith, N. G., & Dukes, J. S. (2013). Plant respiration and photosynthesis in global-scale models: Incorporating acclimation to temperature and CO_2. *Global Change Biology*, *19*(1), 45–63. https://doi.org/10.1111/j.1365-2486.2012.02797.x

Smith, N. G., & Dukes, J. S. (2017). Short-term acclimation to warmer temperatures accelerates leaf carbon exchange processes across plant types. *Global Change Biology*, *23*(11), 4840–4853. https://doi.org/10.1111/gcb.13735

Smith, N. G., & Keenan, T. F. (2020). Mechanisms underlying leaf photosynthetic acclimation to warming and elevated CO_2 as inferred from least-cost optimality theory. *Global Change Biology*.

Smith, N. G., Keenan, T. F., Colin Prentice, I., Wang, H., Wright, I. J., Niinemets, Ü., et al. (2019). Global photosynthetic capacity is optimized to the environment. *Ecology Letters*. https://doi.org/10.1111/ele.13210

Smith, N. G., Lombardozzi, D., Tawfik, A., Bonan, G., & Dukes, J. S. (2017). Biophysical consequences of photosynthetic temperature acclimation for climate. *Journal of Advances in Modeling Earth Systems*, *9*(1), 536–547. https://doi.org/10.1002/2016ms000732

Smith, N. G., Malyshev, S. L., Shevliakova, E., Kattge, J., & Dukes, J. S. (2016). Foliar temperature acclimation reduces simulated carbon sensitivity to climate. *Nature Climate Change*, *6*(4), 407–411. https://doi.org/10.1038/nclimate2878

Still, C. J., Berry, J. A., Collatz, G. J. & DeFries, R. S. (2009). ISLSCP II C4 Vegetation Percentage. In Hall, G. Forrest, G. Collatz, B. Meeson, S. Los, E. Brown de Colstoun, & D. Landis (Eds.), *ISLSCP Initiative II Collection*. [Data set]. Available on-line [http://daac.ornl.gov/] from Oak Ridge National Laboratory Distributed Active Archive Center, Oak Ridge, Tennessee, USA. http://dx.doi.org/10.3334/ORNLDAAC/932

Thornton, P., Lamarque, J., Rosenbloom, N., & Mahowald, N. (2007a). Effects of terrestrial carbon-nitrogen cycle coupling on climate-carbon cycle dynamics. *Global Biogeochemical Cycles*, *21*. https://doi.org/10.1029/2006gb002868

Thornton, P., Lamarque, J.-F., Rosenbloom, N., & Mahowald, N. (2007b). Influence of carbon-nitrogen cycle coupling on land model response to CO_2 fertilization and climate variability. *Global Biogeochemical Cycles*, *1221*. https://doi.org/10.1029/2006gb002868

Von Caemmerer, S. (2000). *Biochemical models of leaf photosynthesis*. Csiro Publishing.

Von Caemmerer, S. (2021). *Updating the steady state model of C_4 photosynthesis*. bioRxiv. https://doi.org/10.1101/2021.03.13.435281. https://www.biorxiv.org/content/early/2021/03/14/2021.03.13.435281

Von Caemmerer, S., & Furbank, R. T. (1999). Modeling C4 photosynthesis. *C4 Plant Biology*, 173–211. https://doi.org/10.1016/b978-012614440-6/50007-0

Wang, H., Prentice, I. C., Keenan, T. F., Davis, T. W., Wright, I. J., Cornwell, W. K., et al. (2017). Towards a universal model for carbon dioxide uptake by plants. *Nature Plants*, *3*(9), 734. https://doi.org/10.1038/s41477-017-0006-8

Way, D. A., & Yamori, W. (2014). Thermal acclimation of photosynthesis: On the importance of adjusting our definitions and accounting for thermal acclimation of respiration. *Photosynthesis Research*, *119*(1–2), 89–100. https://doi.org/10.1007/s11120-013-9873-7

Wherley, B. G., & Sinclair, T. R. (2009). Differential sensitivity of C_3 and C_4 turfgrass species to increasing atmospheric vapor pressure deficit. *Environmental and Experimental Botany*, *67*(2), 372–376. https://doi.org/10.1016/j.envexpbot.2009.07.003

Wieder, W., Cleveland, C., Smith, W., & Todd-Brown, K. (2015). Future productivity and carbon storage limited by terrestrial nutrient availability. *Nature Geoscience*, *8*, 441–444. https://doi.org/10.1038/ngeo2413

Wolf, J., & Ziska, L. (2018). Comment on "unexpected reversal of C_3 versus C_4 grass response to elevated CO_2 during a 20-year field experiment". *Science*, *361*(6402). https://doi.org/10.1126/science.aau1073

Wright, I., Reich, P., & Westoby, M. (2003). Least-cost input mixtures of water and nitrogen for photosynthesis. *The American Naturalist*, *161*, 98–111. https://doi.org/10.1086/344920

Yamori, W., Hikosaka, K., & Way, D. A. (2014). Temperature response of photosynthesis in C_3, C_4, and cam plants: Temperature acclimation and temperature adaptation. *Photosynthesis Research*, *119*(1–2), 101–117. https://doi.org/10.1007/s11120-013-9874-6

Zaehle, S., & Friend, A. (2010). Carbon and nitrogen cycle dynamics in the o-cn land surface model: 1. Model description, site-scale evaluation, and sensitivity to parameter estimates. *Global Biogeochemical Cycles*, *24*(1). https://doi.org/10.1029/2009gb003521

Zhou, H., Helliker, B. R., Huber, M., Dicks, A., & Akçay, E. (2018). C_4 photosynthesis and climate through the lens of optimality. *Proceedings of the National Academy of Sciences*, *115*(47), 12057–12062. https://doi.org/10.1073/pnas.1718988115

Zhu, Q., Riley, W. J., Tang, J., Collier, N., Hoffman, F. M., Yang, X., & Bisht, G. (2019). Representing nitrogen, phosphorus, and carbon interactions in the e3sm land model: Development and global benchmarking. *Journal of Advances in Modeling Earth Systems*, *11*(7), 2238–2258. https://doi.org/10.1029/2018ms001571